J. Ocean Univ. China (Oceanic and Coastal Sea Research)
https://doi.org/10.1007/s11802-021-4692-5
ISSN 1672-5182, 2021 20 (4): 949-958
http://www.ouc.edu.cn/xbywb/
E-mail:xbywb@ouc.edu.cn

Comparative Transcriptome Analysis of Heart Tissue in Response to Hypoxia in Silver Sillago (*Sillago sihama*)

SAETAN Wanida, YE Minghui, LIN Xinghua, LIN Xiaozhan, ZHANG Yulei, HUANG Yang, DU Tao, LI Guangli, and TIAN Changxu*

Fisheries College, *Guangdong Ocean University*, *Guangdong Research Center on Reproductive Control and Breeding Technology of Indigenous Valuable Fish Species*, *Guangdong Provincial Engineering Laboratory for Mariculture Organism Breeding*, *Southern Marine Science and Engineering Guangdong Laboratory*, *Zhanjiang* 524088, *China*

(Received July 25, 2020; revised October 15, 2020; accepted December 8, 2020)

Abstract *Sillago sihama*, commonly known as silver sillago, is considered as an economically important fish species in China. It is sensitive to hypoxia stress in the larval stage, and the mechanism has not been understood thoroughly. In this study, we investigated the transcriptome change in heart tissues under hypoxia stress. The fish were divided into four groups, including 1 h of hypoxia (hypoxia1h, dissolved oxygen (DO) = 1.5 ± 0.1 mg L^{-1}), 4 h of hypoxia (hypoxia4h, DO = 1.5 ± 0.1 mg L^{-1}), 4 h of reoxygen (reoxygen4h, DO = 8.0 ± 0.2 mg L^{-1}) after 4 h of hypoxia (DO = 1.5 mg L^{-1}) and normoxia or control (DO = 8.0 ± 0.2 mg L^{-1}) groups. The results showed that a total of 3068 genes were identified as differentially expressed genes (DEGs) based on the criteria $|\log_2(\text{Fold change})| > 1.0$ and adjusted *P*-value < 0.05. A total of 7761141 and 1151 DEGs were obtained from hypoxia1h, hypoxia4h and reoxygen4h groups, respectively. The enrichment pathway analysis showed that the DEGs were significantly enriched in ribosome biogenesis in eukaryotes, retinol metabolism, DNA replication and the oxidative phosphorylation (OXPHOS) pathways. Thirteen DEGs from the RNA-seq results were validated by quantitative real-time polymerase chain reaction (qRT-PCR). These candidate genes are considered as important regulatory factors involved in the hypoxia stress response in *S. sihama*.

Key words transcriptomes; heart tissues; hypoxia stress; *Sillago sihama*; gene expression

1 Introduction

Hypoxia is considered as poor solubility of dissolved oxygen (DO) (< 2.0 mg L^{-1}), which frequently occurs in aquaculture (Han *et al*., 2018). Due to global warming and eutrophication, hypoxia in the aquatic environment has become one of the most critical factors of aquaculture loss (Lai *et al*., 2016; Li *et al*., 2018). The hypoxia stress induces both chronic and acute stress responses in fish, which directly affects fish embryogenesis, immunology and growth physiology. For example, three-spine stickleback (*Gasterosteus aculeatus*) embryos showed delayed development and increased mortalities under hypoxia stress (Fitzgerald *et al*., 2017). Hypoxia stress decreased the fertility of Gulf killifish (*Fundulus grandis*) and common carp (*Cyprinus carpio*) (Landry *et al*., 2007; Wu *et al*., 2017). The molecular mechanisms of fish response to hypoxia stress have become a research hotspot in recent years. The anaerobic and metabolism system in zebrafish (*Danio rerio*) were quickly changed after exposure to hypoxia (Martinovic *et al*., 2009). The expression of immune system-related genes was found to be down-regulated due to acute hypoxia in Nile tilapia (*Oreochromis niloticus*) (Choi *et al*., 2007). In addition, differentially expressed genes and their regulatory pathways related to hypoxia stress tolerance were observed in various fish species, such as Nile tilapia (Li *et al*., 2017), blunt snout bream (*Megalobrama amblycephala*) (Chen *et al*., 2017), eelpout (*Zoarces viviparus*) (Asker *et al*., 2013), Asian Seabass (*Lates calcarifer*) (Xia *et al*., 2013) and fugu (*Takifugu rubripes*) (Jiang *et al*., 2017).

Silver sillago (*Sillago sihama*) is one of the common species of Sillaginidae family (Tian *et al*., 2019). It is one of the main tropical shallow fish species, which is generally distributed in the Indian Ocean and along the coasts of China and Southeast Asia (Saetan *et al*., 2020). This fish species is nutritious and delicious, with a high economic value (Li *et al*., 2019). Due to overfishing, the population of *S. sihama* has decreased dramatically in recent years. Also, the poor hypoxic tolerance of this species limits the scale of artificial breeding of *S. sihama* (Gunn *et al*., 1985). Up to date, a number of studies have been conducted in *S. sihama* on the morphology (Tongnunui *et al*., 2010), reproductive biology and artificial breeding (Yoshioka, 2000), population genetics (GUO *et al*., 2014; Li *et al*., 2019), and tissue physiology and ecology (Hakimelahi *et al*., 2012).

* Corresponding author. Tel: 0086-18406683455
E-mail: tiancx@gdou.edu.cn

We have conducted the transcriptome analysis of *S. sihama* gill and liver tissues response to hypoxia stress, finding that the expression patterns of hypoxia-related genes were tissue-specific, and further study is necessary in more tissues (Saetan *et al.*, 2020; Tian *et al*., 2020).

Transcriptome sequencing technology has been widely used for quantitative and qualitative analysis of transcripts in cells. In recent years, different candidate genes related to hypoxia and their signal transduction pathways have been identified based on RNA-seq technology in many fish species, including the blunt snout bream (Chen *et al*., 2017), Nile tilapia (Li *et al.*, 2017), schizothoracine fish (*Gymnocypris eckloni*) (Qi *et al*., 2018) and crucian carp (*Carassius auratus*) (Liao *et al*., 2013). In a previous study, it was observed the cytochrome P450 (CYP) and glutathione S-transferase (GST) gene families were widely expressed under hypoxia stress (Saetan *et al*., 2020). In teleosts, the heart is the organ in response to the changes of DO level in water, but the molecular mechanisms are still unclear.

In this study, transcriptome analysis was performed on heart tissue in *S. sihama*. Furthermore, quantitative real-time polymerase chain reaction (qRT-PCR) was used to verify the expression of selected genes. Our study will provide valuable information to understand the molecular mechanisms of *S. sihama* heart response to hypoxia stress.

2 Materials and Methods

2.1 Fish and Hypoxia Experimental Conditions

Healthy adult *S. sihama* (13.40 cm ± 1.05 cm of total length and 14.57 g ± 3.17 g of body weight) were obtained from Donghai Island, Guangdong, China. The fish were maintained in fiber tanks with a bio-filtered water circulation system at 25℃ for 1 month. The fish were fed with a commercial diet twice per day. The water quality was checked every day, and the dead animals and particles were removed at once. During the test period, the water temperature was maintained at 25℃ ± 1℃, dissolved oxygen (DO) at (8.0 ± 0.5) mg L^{-1} (normoxia) and the salinity at 29.

The experiment methods were the same as described previously (Saetan *et al*., 2020). Healthy fish were randomly selected and transferred to four aquarium tanks (50-L) at a density of 50 fish per tank. Each tank contained 40 L of seawater. During hypoxia stress period, the concentration of DO was continuously monitored each hour by JPB-607A dissolved oxygen meter (INESA Scientific Instrument Co. Ltd., Shanghai, China). The fish were randomly divided into four groups, including hypoxia for 0 h (normoxia, DO = 8.0 ± 0.2 mg L^{-1}), hypoxia for 1 h (hypoxia1h, DO = 1.5 ± 0.1 mg L^{-1}), hypoxia for 4 h (hypoxia4h, DO = 1.5 ± 0.1 mg L^{-1}) and normal oxygen recovered in 4 h after hypoxia4h (reoxygen4h, DO = 8.0 ± 0.2 mg L^{-1}). At each time point, fish heart sample was collected, immediately frozen in liquid nitrogen, and stored at −80℃ for further analysis.

2.2 RNA Extraction and Sequencing

The total RNA extraction and sequence preparing methods used in this study was described previously by Saetan *et al*. (2020). Total RNA of heart tissue (n=3 per group) from four groups was extracted with TRIzol reagent (Life Technologies, Carlsbad, CA, USA) following the manufacturer's instructions. Purified RNA samples were indicated by A260/A280 ratios ranging from 2.0 to 2.2 with NanoPhotometer spectrophotometer (Nanodrop 2000c, Thermo Scientific, Wilmington, DE, USA). RNA integrity samples were obtained by ethidium bromide staining of 28S and 18S ribosomal bands on a 1.0% agarose gel. The high-quality RNA samples were used to generated cDNA libraries using the NEBNext® Ultra™ RNA Library Prep Kit for Illumina® (NEB, USA) following the manufacturer's instructions. A total of 3 μg RNA was prepared for each Illumina library. The libraries were sequenced on the HiSeq platform with 150 bp sequenced from both ends (paired-end). The RNA-Seq data were uploaded to Sequence Read Archive database (SRA) (Accession no.: SRR 9651325-SRR9651336).

2.3 Data Analysis

Data filtering, reads mapping and differential expression analysis were conducted in accordance with the methods of Saetan *et al.* (2020). The assembled *S. sihama* genome (Lin *et al*., 2021) was used as a reference genome for mapping reads. The genome assembly included 521.63 Mb in 551 contigs with a contig N50 of 13559141 bp. An index of the reference genome was built, and the paired-end clean reads were aligned to the reference genome using Hisat2 v2.0.5. The gene expression levels were estimated by fragments per kilobase of exon model per million reads mapped (FPKM) (Trapnell *et al*., 2010). Clean data (clean reads) were picked out by removing reads containing adapter, poly-N and low-quality reads from raw data which were processed through in-house perl scripts. DESeq2 R package (version 1.16.1) was used to identify differentially expressed genes (DEGs) between the normoxia and hypoxia groups (Varet *et al*., 2016) with the threshold of $|\log_2(\text{Fold change})| > 1.0$ and Padj < 0.05 (Anders *et al*., 2010). The DEGs were further mapped to the Kyoto Encyclopedia of Genes and Genomes (KEGG) database (http://www.genome.jp/kegg/) and Gene Ontology (GO) database (Padj ≤ 0.05).

2.4 qRT-PCR Validation

A total of 13 DEGs were randomly selected from hypoxia1h *vs*. normoxia, hypoxia4h *vs*. normoxia, and reoxygenation4h *vs*. normoxia to verify the expression of DEGs. Thirteen DEGs included 5 genes of co-expression in hypoxia group, 6 genes of hypoxia-related gene and 2 genes of top up- or down-regulated expressed (Table 1). The primers of all selected genes were designed using Primer Premier software v6.0 and listed in Table 1. qRT-PCR was performed using SYBR Green qPCR Mix (Dongsheng Biotech, Guangzhou, China) on a LightCycler real-time quantitative PCR system (Roche, USA) according to the manufacturer's instructions. The ribosomal protein L7 (*rpl7*) gene was used as a reference to standardize gene expression

Table 1 PCR primer sequences

No	Gene name	Primer name	Sequence (5'-3')
1	*Ddit4*	*Ddit4-f*	ACCAGAGCAGCAGGAGTGAGAC
		Ddit4-r	TCCACGCAGAGGTCGATGAGAG
2	*Igf2*	*Igf2-f*	AGAGCGGAGAGCAGCAGAATGA
		Igf2-r	CTTGGCGGGTTTGGCACAGT
3	*Vlc3ocal*	*Vlc3ocal-f*	GGACCATTGCAGTTGACTTTG
		Vlc3ocal-r	TTTGGACCTCTCAGCCATTC
4	*Hspal*	*Hspal-f*	ACAGATACAAAGCCGAGGATG
		Hspal-r	GGTGCTGGTACTCCTCTTTATC
5	*Tpm3*	*Tpm3-f*	AGCCCATCAAACCTCAGCCAAA
		Tpm3-r	GCATCCTTCAGAGCCTCAGAGT
6	*Actc1*	*Actc1-f*	GAGCACGGCATCATCACCAACT
		Actc1-r	CCATCACCAGCATCCAGCACAA
7	*Myh*	*Myh-f*	GCAGTATGAGGAGGAGCAGGAG
		Myh-r	CGAGGACAGAAGCCAGAGCATT
8	*Egln3*	*Egln3-f*	GCTGGAGCAGGTGAAGGAGATG
		Egln3-r	TCGATGAGCGTGAGCAGGAAG
9	*Hif1an*	*Hif1an-f*	CGCATTACGACGAGCAACAGAA
		Hif1an-r	GCCGCCATTCAACAGTGATTCA
10	*Hsp70a*	*Hsp70a-f*	CGACAGATACAAAGCCGAAGA
		Hsp70a-f	GGTGCTGGTACTCCTCTTTATC
11	*Epo*	*Epo-f*	ACCGTCCGCCAGCAGATGAA
		Epo-r	TCGTCACCAGCCAGGAAGCA
12	*Aldoc*	*Aldoc-f*	ACCAAGTACAGCGGCGAGGA
		Aldoc-r	GGCGAGCGGACAGTTGTTAATG
13	*Egln1*	*Egln1-f*	GTAGGTGCCGCAGCTCCTTCTA
		Egln1-r	CGCTCTCCTCCGACTCTTGACT
14	*rpl7*	*rpl7-f*	GCAAAGTGACCAGGAAACTGAT
		rpl7-r	GGCTGACACCGTTGATACCTCT

values (Zhang *et al*., 2018). All PCRs amplification were performed in triplicate. Relative expression levels were measured in terms of threshold cycle value and normalized using the $2^{-\Delta\Delta Ct}$ method (Livak *et al*., 2001).

3 Results

3.1 Illumina Sequencing Assembly

Twelve cDNA libraries from four groups with triplicates were sequenced by Illumina technology to investigate the transcriptomes of heart tissues during hypoxia stress (Table 2). A total of 62932232 raw reads were obtained. A total of 159436408, 168800258, 143631922 and 136793080 clean reads were obtained from hypoxia1h, hypoxia4h, reoxygen4h and normoxia group, respectively after removing low-quality reads. All Q20 and Q30 values of the read sequences in the samples exceeded 96.22% and 90.72%, respectively.

3.2 Identification and Annotation of DEGs

In total 3068 DEGs were identified, of which 776, 1141 and 1151 DEGs were obtained from hypoxia1h, hypoxia4h and reoxygen4h groups, respectively. The number of significantly up-regulated genes in hypoxia1h, hypoxia4h and reoxygen4h groups were 387, 478 and 446, respectively. The number of down-regulated genes were 389, 663 and 705, respectively ($P<0.05$) (Table 3). Further analysis showed that only 136 genes were expressed in different hypoxia groups as compared to the normoxia group (Fig.1). The top ten up- and down-regulated genes were presented in Table 4. Interestingly, the expression of heat shock protein 30 (*Hsp30*) and heat shock protein 70 (*Hsp70*) were shown to be strongly up-regulated under hypoxia stress. Additionally, cardiac muscle genes including troponin C (*TnnC*), troponin I (*TnnI*), tropomyosin (*Tpm3*) and

Table 2 Summary of heart transcriptome sequencing data of *S. sihama*

Group		Raw reads	Clean reads	Clean bases (G)	Q20 (%)	Q30 (%)
Hypoxia1h	H_HI_1	50075220	46877360	7.03	96.96	92.25
	H_HI_2	62932232	59122324	8.87	96.86	92.07
	H_HI_3	56671296	53436724	8.02	96.78	91.87
Hypoxia4h	H_HT_1	51760456	49986188	7.50	96.90	92.13
	H_HT_2	64823468	62422530	9.36	96.70	91.68
	H_HT_3	58403890	56391540	8.46	96.93	92.20
Reoxygen4h	H_RO_1	45656232	43242344	6.49	96.51	91.26
	H_RO_2	56663266	54220512	8.13	96.59	91.40
	H_RO_3	49397030	46169066	6.93	96.34	90.91
Normoxia (control)	H_NO_1	45220424	42731628	6.41	96.61	91.51
	H_NO_2	43067234	41194778	6.18	96.22	90.72
	H_NO_3	55349350	52866674	7.93	96.62	91.51

Notes: Q20, percentage of bases for which the Phred value is > 20; Q30, percentage of bases for which the Phred value is > 30.

Table 3 Summary of differentially expressed genes (DEGs) in *S. sihama* based on the criteria $|\log_2(\text{Fold change})| > 1.0$ and Padj < 0.05

DEGs	Hypoxia1h	Hypoxia4h	Reoxygen4r
Up-regulated	387	478	446
Down-regulated	389	663	705
Total	776	1141	1151

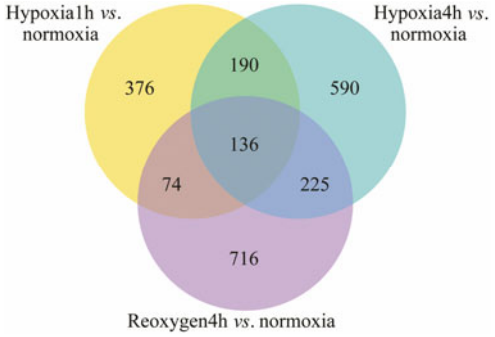

Fig.1 Analysis of differentially expressed genes (DEGs). Venn diagram of corresponding significantly up-regulated or down-regulated genes in hypoxia1h, hypoxia4h and reoxygen4h groups compared to the normoxia group ($\log_2(\text{Fold chang}) > 1.0$ and Padj < 0.05).

Table 4 Top 20 differentially expressed genes (DEGs) in the heart of *S. Sihama*

	Gene symbol	Log_2 (Fold change)	Gene name
Hypoxia1h *vs*. normoxia	*LOC107576620*	8.430	Uncharacterized protein
	Epd1	7.383	Ependymin-1
	Klhl40b	6.960	Kelch-like protein 40b
	Hsp30	6.547	Heat shock protein 30
	LOC104918974	5.817	Uncharacterized protein
	Klhl40a	5.022	Kelch-like protein 40a
	Ptprn	4.800	Receptor-type tyrosine-protein phosphatase N
	Tac1	4.295	Tachykinin 1
	Ism2	4.090	Isthmin-2
	Asgr2	3.896	Asialoglycoprotein receptor 2
	Gabrg3	−7.531	Gamma-aminobutyric acid receptor subunit gamma-3
	Rpa2-a	−5.569	Replication protein A 32 kDa subunit-A
	Zp3	−4.802	Zona pellucida sperm-binding protein 3
	Tpm3	−4.549	Tropomyosin 3
	Lrp4	−4.269	Lipoprotein receptor-related protein 4
	Tnni2	−4.247	Troponin I, fast skeletal muscle
	Myh	−3.859	Myosin heavy chain
	Nadsyn1	−3.391	NAD^+ synthase (glutamine hydrolysing)
	Ppef2	−3.297	Serine/threonine-protein phosphatase with EF-hands
	Mybpc2	−3.260	Myosin-binding protein C, fast-type
Hypoxia4h *vs*. normoxia	*Pif1*	6.624	ATP-dependent DNA helicase PIF1
	Hsp30	6.460	Heat shock protein 30
	Chla	6.272	Chitinase
	Natt3	5.765	Natterin-3
	LOC104918974	5.742	Uncharacterized protein
	Pcdhd2	4.977	Protocadherin delta 2
	Slc16a3	4.846	Solute carrier family 16 member 3
	LOC109081681	4.769	Uncharacterized protein
	Hsp70	4.504	Heat shock protein 70
	Rnf223	4.143	RING finger protein 223
	LOC103908802	−6.660	Uncharacterized protein
	Mylpf	−5.273	Fast skeletal myosin light chain 2
	Tnnc2	−4.722	Troponin C, skeletal muscle
	Klhl38	−4.675	Kelch-like protein 38
	Slc25a4	−4.661	Solute carrier family 25 member 4
	Atp2a1	−4.637	Ca^{2+} transporting ATPase
	Ccnb2	−4.622	G2/mitotic-specific cyclin-B2
	Tmem26	−4.606	Transmembrane protein 26
	Tpm3	−4.570	Tropomyosin 3
	Prss27	−4.531	Serine protease 27
Reoxygen4h *vs*. normoxia	*LOC109203576*	6.973	Uncharacterized protein
	Hsp30	5.338	Heat shock protein 30
	Asgr2	4.098	Asialoglycoprotein receptor 2
	Prrt3	4.084	Proline-rich transmembrane protein 3
	Srrm3	3.745	Arginine repetitive matrix 3
	Rnf223	3.734	RING finger protein 223
	Mhc1	3.412	Major histocompatibility complex, class I
	Ctrc	3.367	Chymotrypsin C
	Edn2	3.289	Endothelin-2
	Prss	3.270	Trypsin
	Tnnc2	−6.561	Troponin C, skeletal muscle
	Atp2a1	−4.923	Ca^{2+} transporting ATPase
	Slc25a4	−4.841	Solute carrier family 25
	Mylpf	−4.753	Fast skeletal myosin light chain 2
	Nr4a3	−4.627	Nuclear receptor subfamily 4
	Tpm3	−4.292	Tropomyosin 3
	Ckm	−4.247	Creatine kinase
	Mybpc2	−3.827	Myosin-binding protein C, fast-type
	Aqp1	−3.764	Aquaporin 1
	LOC108878457	−3.739	Uncharacterized protein

myosin heavy chain (*Myh*) were significantly down-regulated.

3.3 GO and KEGG Enrichment Analyses of DEGs

The DEGs were classified into three major functions, including biological process (BP), cellular component (CC) and molecular function (MF) according to GO enrichment analysis. The GO terms of DEGs in each group were shown in Table 5. Among significantly top 30 BP terms ($P<0.05$), the BP terms were mostly enriched to ribosome biogenesis (GO:0042254) and DNA replication initiation (GO:0006270). The majority of DEGs in the CC terms were related to the cytoskeleton (GO:0005856), actin cytoskeleton (GO:0015629) and cytoskeletal part (GO:0044430). In the MF terms, the DEGs were significantly enriched to heme binding (GO:0020037) and tetrapyrrole binding (GO:0046906) (Table 5).

KEGG pathway analysis was annotated to obtain significantly enriched pathways. There were 3 KEGG pathways, including ribosome biogenesis in eukaryotes, retinol metabolism and DNA replication pathways, which were significantly enriched in the hypoxia1h group (Table 6). In

Table 5 Gene Ontology (GO) enrichment of differentially expressed genes (DEGs)

	GO:ID	Description	Term type	Number of gene	P_{adj}
Hypoxia1h group	GO:0042254	Ribosome biogenesis	BP	8	8.49E-04
	GO:0006270	DNA replication initiation	BP	5	1.79E-03
	GO:0022613	Ribonucleoprotein complex biogenesis	BP	8	1.86E-03
	GO:0006260	DNA replication	BP	9	2.95E-03
	GO:0006261	DNA-dependent DNA replication	BP	5	3.35E-03
	GO:0005861	Troponin complex	CC	6	7.97E-04
	GO:0005865	Striated muscle thin filament	CC	6	7.97E-04
	GO:0030016	Myofibril	CC	6	7.97E-04
	GO:0030017	Sarcomere	CC	6	7.97E-04
	GO:0036379	Myofilament	CC	6	7.97E-04
	GO:0043292	Contractile fiber	CC	6	7.97E-04
	GO:0044449	Contractile fiber part	CC	6	7.97E-04
	GO:0015629	Actin cytoskeleton	CC	10	3.77E-02
	GO:0099080	Supramolecular complex	CC	8	3.77E-02
	GO:0099081	Supramolecular polymer	CC	8	3.77E-02
	GO:0099512	Supramolecular fiber	CC	8	3.77E-02
Hypoxia4h group	GO:0005861	Troponin complex	CC	7	4.67E-04
	GO:0005865	Striated muscle thin filament	CC	7	4.67E-04
	GO:0030016	Myofibril	CC	7	4.67E-04
	GO:0030017	Sarcomere	CC	7	4.67E-04
	GO:0036379	Myofilament	CC	7	4.67E-04
	GO:0043292	Contractile fiber	CC	7	4.67E-04
	GO:0044449	Contractile fiber part	CC	7	4.67E-04
	GO:0015629	Actin cytoskeleton	CC	16	4.67E-04
	GO:0071944	Cell periphery	CC	14	7.87E-04
	GO:0044430	Cytoskeletal part	CC	22	1.09E-03
	GO:0099080	Supramolecular complex	CC	12	1.93E-03
	GO:0099081	Supramolecular polymer	CC	12	1.93E-03
	GO:0099512	Supramolecular fiber	CC	12	1.93E-03
	GO:0005856	Cytoskeleton	CC	23	2.89E-03
	GO:0005886	Plasma membrane	CC	11	6.41E-03
	GO:0005887	Integral component of plasma membrane	CC	6	1.56E-02
	GO:0031226	Intrinsic component of plasma membrane	CC	6	1.56E-02
	GO:0016459	Myosin complex	CC	9	4.10E-02
	GO:0020037	Heme binding	MF	14	4.75E-02
	GO:0046906	Tetrapyrrole binding	MF	14	4.75E-02
Reoxygen4h group	GO:0031090	Organelle membrane	CC	12	6.85E-03
	GO:0098798	Mitochondrial protein complex	CC	6	1.50E-03
	GO:0044455	Mitochondrial membrane part	CC	7	8.58E-04
	GO:0098800	Inner mitochondrial membrane protein complex	CC	6	8.58E-04
	GO:0044429	Mitochondrial part	CC	12	2.53E-04
	GO:0031967	Organelle envelope	CC	12	2.05E-04
	GO:0031975	Envelope	CC	12	2.05E-04
	GO:0005739	Mitochondrion	CC	14	2.05E-04
	GO:0005740	Mitochondrial envelope	CC	12	1.73E-04
	GO:0005743	Mitochondrial inner membrane	CC	9	1.73E-04
	GO:0019866	Organelle inner membrane	CC	9	1.73E-04
	GO:0031966	Mitochondrial membrane	CC	11	1.73E-04

Table 6 The significant enrichment of Kyoto Encyclopedia of Genes and Genomes (KEGG) pathways of treatment groups

Group	Pathway	Pathway ID	Sample number	Up-regulated	Down-regulated	Class	Sub-categories	Corrected *P* value
Hypoxia1h group	Ribosome biogenesis in eukaryotes	dre03008	13	13	0	Genetic information processing	Translation	2.83E-07
	Retinol metabolism	dre00830	6	3	3	Metabolism	Metabolism of cofactors and vitamins	2.40E-04
	DNA replication	dre03030	6	6	0	Genetic information processing	Replication and repair	1.22E-03
Reoxygen4h group	Oxidative phosphorylation	dre00190	27	1	26	Metabolism	Energy metabolism	4.93E-13

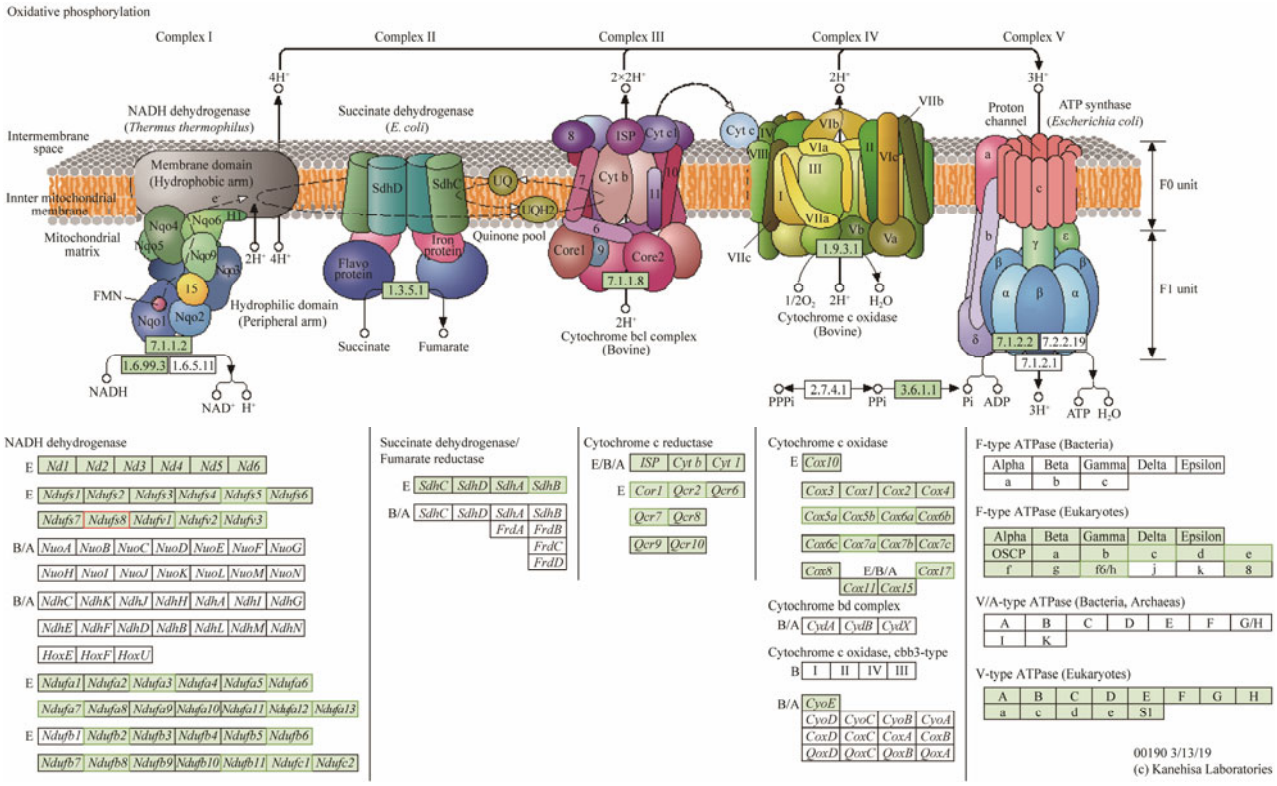

Fig.2 Effect of hypoxia on the oxidative phosphorylation pathway. The green frames represent the genes were up-regulated, while the red frames represent that the genes were down-regulated, respectively.

addition, the oxidative phosphorylation pathway (Fig.2) was significantly enriched in the reoxygen4h group. There was no KEGG pathway significantly enriched in the hypoxia-4h group (Table 6).

3.4 Validation of Gene Expression Levels

A total of 13 DEGs were selected and analyzed using qPCR (Fig.3). Our results demonstrated that the changing trends of those genes from q-PCR were similar to the results from RNA-seq expression analysis, which supported the reliability of the transcriptome data.

4 Discussion

Hypoxia is a common phenomenon that frequently occurred in aquatic environment. It severely affects various physiological functions in fish, such as metabolism and cardiovascular regulation (Abdel-Tawwab *et al.*, 2019). The fishes have evolved various adaptation methods to hypoxia stress through a complex suite of molecular regulation (Qi *et al.*, 2018). It was showed that the gill and liver tissues of *S. sihama* responded to rapid changes of the DO level in water, while the expression patterns of hypoxia-related genes were tissue-specific (Saetan *et al.*, 2020; Tian *et al.*, 2020). Thus it is necessary to carry out research on hypoxia in more tissues. The heart is one of the major organs for fish to sense changes of DO level (Mu *et al.*, 2020). Hypoxia stress usually reduces the rate of pumping oxygen-rich blood to various organs in the body (Nemtsas *et al.*, 2010; Incardona *et al.*, 2016). Therefore, we conducted a comparative transcriptome analysis of *S. sihama* heart tissue under hypoxia stress to understand the molecular mechanisms of heart tissue's response to hypoxia stress.

In the present study, numbers of down-regulated DEGs were increased with the increase of exposure time to hypoxia, which was in agreement with a previous study (Geng *et al.*, 2014). A series of down-regulated DEGs, such as *TnnC*, *TnnI*, *Tpm3* and *Myh*, are associated with cardiac muscle function, demonstrating that the fish heart responds to external environmental stress by down-regulating the

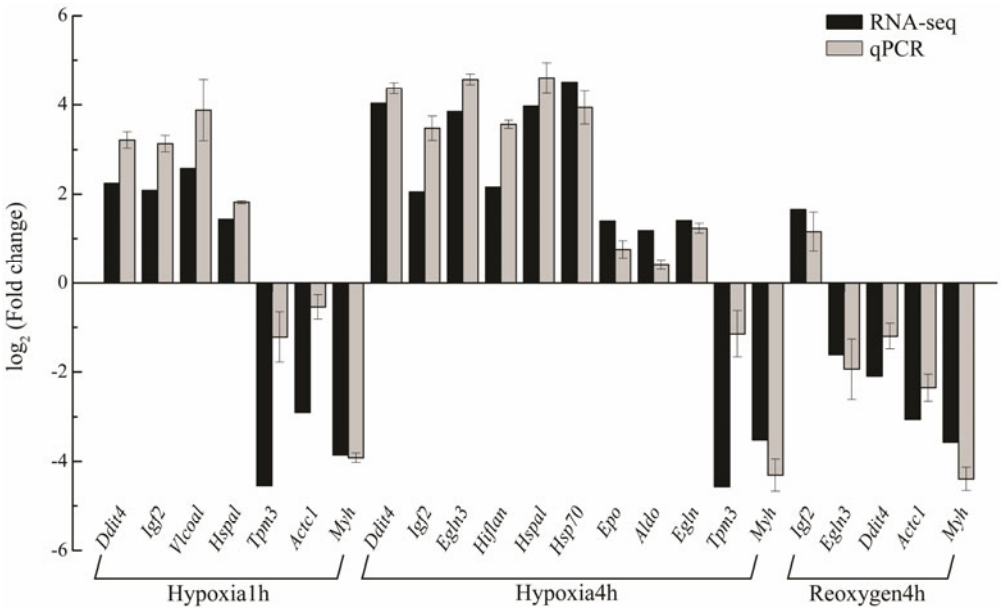

Fig.3 Comparison of gene expression data between RNA-seq and quantitative real-time PCR (qRT-PCR) after hypoxia acclimation compared to the normoxia. The *x*-axis presents the gene name and the *y*-axis presents fold change in gene expression. All data represent the mean value of three biological replicates. Error bars represent the standard errors of three replicates. Statistically significant differences from control are presented, with * $P<0.05$.

gene expression levels related to energy metabolism. *Tnn* was a complex of skeletal and cardiac muscle thin filaments, which consists of three subunits, including *TnnI*, *TnnT* and *TnnC*. *Tnn* plays an important role in muscle activity and changing intracellular Ca^{2+} concentration (Katrukha *et al*., 2013). *Tpm3* is a component of thin muscle that is associated with cardiac muscle activation (Marston, 2008; Bai *et al*., 2013). *Myh* converts the chemical energy of Adenosine triphosphate (ATP) to mechanical energy in eukaryotic cells (Liang *et al*., 2007). All of these genes are associated with stress response in cardiac muscle (Mizbani *et al*., 2016; Stelzle *et al*., 2018), and play a pivotal role in predicting the expression of heart failure in patients. The heart of *S. sihama* can also respond to hypoxia stress through changes in the gene expression levels related to energy metabolism and oxygen consumption.

The detoxification proteins, heat shock protein 30 (*Hsp30*) and heat shock protein 70 (*Hsp70*) were significantly up-regulated under hypoxia stress. Heat shock proteins (*Hsps*) are important to protect cells and prevent aggregation of proteins (Junprung *et al*., 2019). Currie *et al.* (2000) reported that *Hsp30* was induced by different environmental stressors, which was involved in the inhibition of apoptosis of cells. *Hsp70* is mainly involved in protecting the cells from extra stress to improve the cell survival. It is used as a bioindicator of cellular stress in animals (Zhou *et al.,* 2019). In this experiment, the expression levels of *Hsp30* and *Hsp70* were significantly up-regulated ($P<0.05$) in *S. sihama* hearts under hypoxic stress, which was in line with the results reported in many fish species (Qian and Xue, 2016; Liu *et al*., 2019; Gao *et al*., 2020). Our results suggested that Hsps 30/70 might play an essential role in protecting the heart tissues of *S. sihama* from hypoxia stress.

In the present study, the functional classification of DEGs was carried out by GO enrichment and KEGG pathway analyses. As showed in Table 6, DEGs were mainly enriched in metabolic (*e.g*., oxidative phosphorylation and retinol metabolism) and genetic information processing-related pathways (*e.g*., ribosome biogenesis in eukaryotes and DNA replication), which were also observed in schizothoracine fish (Qi *et al*., 2018), blue tilapia (*Oreochromis aureus*) (Nitzan *et al*., 2019) and blunt snout bream (Chen *et al*., 2017) under hypoxia stress, suggesting that these categories pathways may play an essential role under hypoxia stress in *S. sihama* as well as other fishes.

ATP is the main source of energy within a cell. ATP is generated in mitochondria by the oxidative phosphorylation (OXPHOS) pathway (Wang *et al*., 2020). OXPHOS is a metabolic process, in which electrons produced by the citric acid cycle are transferred to the mitochondrial respiratory complexes (Silva-Marrero *et al*., 2017; Luo *et al*., 2019; Wang *et al*., 2020). This pathway is also involved in multiple cellular processes, such as calcium homeostasis, cyclic adenosine monophosphate (cAMP)/protein kinase A (PKA) signaling, inflammation, reactive oxygen species (ROS) production and apoptosis (Bergman and Ben-Shachar, 2016). Our study showed that most of the DEGs in OXPHOS pathway were down-regulated (Fig.2), suggesting that the OXPHOS pathway in heart tissue was suppressed by hypoxia stress. Fourteen DEGs related to Nicotinamide adenine dinucleotide (NADH) dehydrogenase were down-regulated in the reoxygen4h group, such as NADH dehydrogenase (ubiquinone) subunit 3 (*Nduf3*), Fe-S protein 1 (*Ndufs1*) and Fe-S protein 2 (*Ndufs2*). The decrease in NADH dehydrogenase expression can promote a stress-adaptive response in different aquatic animals under different stress conditions (Olsvik *et al*., 2013; Chakrapani *et al*., 2016; Mohapatra *et al*., 2018), demonstrating that the OXPHOS pathway plays a vital role in fish adapt-

ing to hypoxic environments.

Retinol metabolism plays an important role in cell signal transduction in embryonic development and adult physiology (Perlmann, 2002; Kam *et al.*, 2012). Excessive retinol can lead to hypoxia and pathological endosteum mineralization in rats (Lind *et al.*, 2011). In this study, several genes, such as retinol dehydrogenase 10 (*Rdh10*), retinal dehydrogenase (*Aldh1a*) and cytochrome P450 27C1 (*Cyp27c1*) were up-regulated. In contrast, the retinol dehydrogenase 8 (*Rdh8*), aldehyde oxidase (*Aox*) and cytochrome P450 26B1 (*Cyp26b1*) genes were down-regulated. The cytochrome P450 (*Cyp*) gene was one of the environmental stress-induced genes, and hypoxia exposure influenced these genes in teleost fishes (Escobar-Camacho *et al*., 2019). The different expression patterns of *Cyp* gene responding to stress were also reported in *S. sihama* (Saetan *et al*., 2020), zebrafish (Ben-Moshe *et al*., 2014) and Nile tilapia (Feng *et al*., 2015). The Aldh1a2 protein, belonging to the aldehyde dehydrogenase (ALDH) family, can catalyze the synthesis of retinoic acid (RA) from retinaldehyde (Li *et al*., 2015). Hypoxia stress can induce the up-regulation of *Aldh1a2* gene expression, which has also been observed in multiple species, including zebrafish (D'Aniello *et al*., 2015), Nile tilapia (Feng *et al*., 2015) and rabbits (*Oryctolagus cuniculus*) (Jackson *et al*., 2011). The genes related to retinol metabolism play an important role in response to hypoxic stress in *S. sihama*, and the mechanism remains to be studied.

Ribosomes are large ribonucleoproteins responsible for translating mRNA into protein complex in cells. The ribosome biogenesis played a crucial role in biological processes, such as cell growth and proliferation (Chaillou *et al*., 2014). Under the hypoxia1h group, many DEGs were significantly up-regulated in ribosome biogenesis of the eukaryotes pathway, including fibrillarin (*Nop1*), NOP58 ribonucleoprotein (*Nop58*) and small nuclear ribonucleoprotein (*Snu13*). These genes were involved in the box C/D snoRNA binding protein and responsible for rRNA modification process (Makimoto *et al*., 2006), demonstrating that the protein synthesis in heart tissues increased under hypoxia stress. Besides, DNA replication pathway was enriched with several up-regulated genes in the hypoxia1h group, such as mini-chromosome maintenance complexes 3, 4, 5 and 6 (*Mcm3*, *Mcm4*, *Mcm5* and *Mcm6*). It had been reported that these genes families were the crucial components for the formation of the pre-replication complex (Wu *et al*., 2012). Consistent with the previous study, these gene families were differently expressed in response to stress in medaka fish (*Oryzias latipes*) (Chatani *et al*., 2016) and Nile tilapia (Kwok *et al*., 2015; Majerska *et al*., 2018). The up-regulation of genes belonging to genetic information processing-related pathway, such as ribosome biogenesis in eukaryotes and DNA replication pathway, indicate that heart tissue needs sufficient energy for blood circulation under hypoxia stress.

5 Conclusions

In our study, heart transcriptome response to hypoxia stress was examined using RNA-Seq technology in *S. sihama*. A total of 3068 DEGs were identified, which represented the strongly down-regulated DEGs involved in the cardiac muscle function. Furthermore, the up-regulated *Hsp30* and *Hsp70* genes were related to hypoxia stress. In addition, several DEGs were enriched in the OXPHOS pathway during hypoxia exposure. Our data revealed that candidate genes are important regulatory factors involved in the hypoxia stress response in *S. sihama*.

Acknowledgements

This study was supported by grants from the National Natural Science Foundation of China (Nos. 41706174 and 31702326), the Natural Science Foundation of Guangdong Province (No. 2019A1515110619), the Department of Education of Guangdong Province (Nos. 2018KQNCX111 and 2019KTSCX060), the College Students' Innovation and Entrepreneurship Project of Guangdong Province (No. CX XL2019138) and the Program for Scientific Research Start-up Funds of Guangdong Ocean University (No. R19026).

References

Abdel-Tawwab, M., Monier, M. N., Hoseinifar, S. H., and Faggio, C., 2019. Fish response to hypoxia stress: Growth, physiological, and immunological biomarkers. *Fish Physiology and Biochemistry*, **45**: 997-1013.

Anders, S., and Huber, W., 2010. Differential expression analysis for sequence count data. *Genome Biology*, **11**: R106.

Asker, N., Kristiansson, E., Albertsson, E., Larsson, D. G. J., and Förlin, L., 2013. Hepatic transcriptome profiling indicates differential mRNA expression of apoptosis and immune related genes in eelpout (*Zoarces viviparus*) caught at Göteborg Harbor, Sweden. *Aquatic Toxicology*, **130-131**: 58-67.

Bai, F., Wang, L., and Kawai, M., 2013. A study of tropomyosin's role in cardiac function and disease using thin-filament reconstituted myocardium. *Journal of Muscle Research and Cell Motility*, **34**: 295-310.

Ben-Moshe, Z., Alon, S., Mracek, P., Faigenbloom, L., Tovin, A., Vatine, G. D., *et al*., 2014. The light-induced transcriptome of the zebrafish pineal gland reveals complex regulation of the circadian clockwork by light. *Nucleic Acids Research*, **42**: 3750-3767.

Bergman, O., and Ben-Shachar, D., 2016. Mitochondrial oxidative phosphorylation system (OXPHOS) deficits in schizophrenia: Possible interactions with cellular processes. *Canadian journal of psychiatry*, **61**: 457-469.

Chaillou, T., Kirby, T. J., and McCarthy, J. J., 2014. Ribosome biogenesis: Emerging evidence for a central role in the regulation of skeletal muscle mass. *Journal of Cellular Physiology*, **229**: 1584-1594.

Chakrapani, V., Patra, S. K., Mohapatra, S. D., Rasal, K. D., Deshpande, U., Nayak, S., *et al*., 2016. Comparative transcriptomic profiling of larvae and post-larvae of *Macrobrachium rosenbergii* in response to metamorphosis and salinity exposure. *Genes and Genomics*, **38**: 1061-1076.

Chatani, M., Morimoto, H., Takeyama, K., Mantoku, A., Tanigawa, N., Kubota, K., *et al*., 2016. Acute transcriptional up-regulation specific to osteoblasts/osteoclasts in medaka fish immediately after exposure to microgravity. *Scientific Reports*, **6**: 39545.

Chen, B. X., Yi, S. K., Wang, W. F., He, Y., Huang, Y., Gao, Z. X., *et al*., 2017. Transcriptome comparison reveals insights into muscle response to hypoxia in blunt snout bream (*Megalobrama amblycephala*). *Gene*, **624**: 6-13.

Choi, K., Lehmann, D. W., Harms, C. A., and Law, J. M., 2007. Acute hypoxia-reperfusion triggers immunocompromise in Nile tilapia. *Journal of Aquatic Animal Health*, **19**: 128-140.

D'Aniello, E., Ravisankar, P., *et al*., 2015. *Rdh10a* provides a conserved critical step in the synthesis of retinoic acid during zebrafish embryogenesis. *PLoS One*, **10**: e0138588.

Escobar-Camacho, D., Pierotti, M. E. R., Ferenc, V., Sharpe, D. M. T., Ramos, E., Martins, C., *et al*., 2019. Variable vision in variable environments: The visual system of an invasive cichlid (*Cichla monoculus*) in Lake Gatun, Panama. *The Journal of Experimental Biology*, **222**: jeb188300.

Feng, R., Fang, L., Cheng, Y., He, X., Jiang, W., Dong, R., *et al*., 2015. Retinoic acid homeostasis through *aldh1a2* and *cyp26a1* mediates meiotic entry in Nile tilapia (*Oreochromis niloticus*). *Scientific Reports*, **5**: 1-12.

Fitzgerald, J. A., Katsiadaki, I., and Santos, E. M., 2017. Contrasting effects of hypoxia on copper toxicity during development in the three-spined stickleback (*Gasterosteus aculeatus*). *Environmental Pollution*, **222**: 433-443.

Gao, X., Jiang, Z., Zhang, S., Chen, Q., Tong, S., Liu, X., *et al*., 2020. Transcriptome analysis and immune-related genes expression reveals the immune responses of *Macrobrachium rosenbergii* infected by *Enterobacter cloacae*. *Fish and Shellfish Immunology*, **101**: 66-77.

Geng, X., Feng, J., Liu, S., Wang, Y., Arias, C., and Liu, Z., 2014. Transcriptional regulation of hypoxia inducible factors alpha (*HIF-α*) and their inhibiting factor (*FIH-1*) of channel catfish (*ictalurus punctatus*) under hypoxia. *Comparative Biochemistry and Physiology−B Biochemistry and Molecular Biology*, **169**: 38-50.

Gunn, J. S., and Milward, N. E., 1985. The food, feeding habits and feeding structures of the whiting species *Sillago sihama* (Forsskål) and *Sillago analis* whitley from townsville, North Queensland, Australia. *Journal of Fish Biology*, **26**: 411-427.

Guo, Y. S., Liu, X. M., Wang, Z. D., Lu, H. S., and Liu, C. W., 2014. Isolation and characterization of microsatellite DNA loci from Naihai cutlassfish (*Trichiurus nanhaiensis*). *Journal of Genetics*, **93**: 109-112.

Han, Z., Lv, C., Xiao, S., Ye, K., Zhang, D., Tsai, H. J., *et al*., 2018. Transcriptome profiling of the abdominal skin of *Larimichthys crocea* in light stress. *Journal of Ocean University of China*, **17**: 344-354.

Incardona, J. P., and Scholz, N. L., 2016. The influence of heart developmental anatomy on cardiotoxicity-based adverse outcome pathways in fish. *Aquatic Toxicology*, **177**: 515-525.

Jackson, B., Brocker, C., Thompson, D. C., Black, W., Vasiliou, K., Nebert, D. W., *et al*., 2011. Update on the aldehyde dehydrogenase gene (*ALDH*) superfamily. *Human Genomics*, **5**: 283-303.

Jiang, J. L., Mao, M. G., Lü, H. Q., Wen, S. H., Sun, M. L., Liu, R. T., *et al*., 2017. Digital gene expression analysis of *Takifugu rubripes* brain after acute hypoxia exposure using next-generation sequencing. *Comparative Biochemistry and Physiology−Part D: Genomics and Proteomics*, **24**: 12-18.

Junprung, W., Norouzitallab, P., De Vos, S., Tassanakajon, A., Nguyen Viet, D., Van Stappen, G., *et al*., 2019. Sequence and expression analysis of *HSP70* family genes in *Artemia franciscana*. *Scientific Reports*, **9**: 1-13.

Kam, R. K. T., Deng, Y., Chen, Y., and Zhao, H., 2012. Retinoic acid synthesis and functions in early embryonic development. *Cell and Bioscience*, **2**: 1-14.

Katrukha, I. A., 2013. Human cardiac troponin complex. structure and functions. *Biochemistry (Moscow)*, **78**: 1447-1465.

Kwok, H. F., Zhang, S. D., McCrudden, C. M., Yuen, H. F., Ting, K. P., Wen, Q., *et al*., 2015. Prognostic significance of minichromosome maintenance proteins in breast cancer. *American Journal of Cancer Research*, **5**: 52-71.

Lai, K. P., Li, J. W., Tse, A. C. K., Cheung, A., Wang, S., Chan, T. F., *et al*., 2016. Transcriptomic responses of marine medaka's ovary to hypoxia. *Aquatic Toxicology*, **177**: 476-483.

Landry, C. A., Steele, S. L., Manning, S., and Cheek, A. O., 2007. Long term hypoxia suppresses reproductive capacity in the estuarine fish, *Fundulus grandis*. *Comparative Biochemistry and Physiology Part A: Molecular & Integrative Physiology*, **148**: 317-323.

Li, H. L., Lin, H. R., and Xia, J. H., 2017. Differential gene expression profiles and alternative isoform regulations in gill of nile tilapia in response to acute hypoxia. *Marine Biotechnology*, **19**: 551-562.

Li, J., Yue, Y., Dong, X., Jia, W., Li, K., Liang, D., *et al*., 2015. Zebrafish *foxc1a* plays a crucial role in early somitogenesis by restricting the expression of *aldh1a2* directly. *Journal of Biological Chemistry*, **290**: 10216-10228.

Li, M., Wang, X., Qi, C., Li, E., Du, Z., Qin, J. G., *et al*., 2018. Metabolic response of Nile tilapia (*Oreochromis niloticus*) to acute and chronic hypoxia stress. *Aquaculture*, **495**: 187-195.

Li, Z., Tian, C., Huang, Y., Lin, X., Wang, Y., Jiang, D., *et al*., 2019. A first insight into a draft genome of silver sillago (*Sillago sihama*) via genome survey sequencing. *Animals*, **9** (10): 756.

Liang, C. S., Kobiyama, A., Shimizu, A., Sasaki, T., Asakawa, S., Shimizu, N., *et al.*, 2007. Fast skeletal muscle myosin heavy chain gene cluster of medaka *Oryzias latipes* enrolled in temperature adaptation. *Physiological Genomics*, **29**: 201-214.

Liao, X., Cheng, L., Xu, P., Lu, G., Wachholtz, M., Sun, X., *et al.*, 2013. Transcriptome analysis of crucian carp (*Carassius auratus*), an important aquaculture and hypoxia-tolerant species. *PLoS One*, **8**: 1-11.

Lind, T., Lind, P. M., Jacobson, A., Hu, L., Sundqvist, A., Risteli, J., *et al.*, 2011. High dietary intake of retinol leads to bone marrow hypoxia and diaphyseal endosteal mineralization in rats. *Bone*, **48**: 496-506.

Liu, X., Shi, H., Liu, Z., Kang, Y., Wang, J., and Huang, J., 2019. Effect of heat stress on heat shock protein 30 (*Hsp30*) mrna expression in rainbow trout (*Oncorhynchus mykiss*). *Turkish Journal of Fisheries and Aquatic Sciences*, **19**: 681-688.

Lin, X., Yang, H., Jiang, D., Chen, H., Deng, S., Zhang, Y., *et al.*, 2021. Chromosomal-level genome assembly of silver sillago (*Sillago sihama*). *Genome Biology and Evolution*, **13** (2): evaa 272.

Livak, K. J., and Schmittgen, T. D., 2001. Analysis of relative gene expression data using real-time quantitative PCR and the $2^{-\Delta\Delta CT}$ method. *Methods*, **25**: 402-408.

Luo, Y., Su, R., Wang, Y., Xie, W., Liu, Z., and Huang, Y., 2019. Schizosaccharomycespombe *Mti2* and *Mti3* act in conjunction during mitochondrial translation initiation. *FEBS Journal*, **286**: 4542-4553.

Majerska, J., Feretzaki, M., Glousker, G., and Lingner, J., 2018. Transformation-induced stress at telomeres is counteracted through changes in the telomeric proteome including SAMHD1. *Life Science Alliance*, **1**: e201800121.

Makimoto, Y., Yano, H., Kaneta, T., Sato, Y., and Sato, S., 2006. Molecular cloning and gene expression of a fibrillarin homolog of tobacco BY-2 cells. *Protoplasma*, **229**: 53-62.

Marston, S., 2008. How does genotype define phenotype? Microphysiology of a tropomyosin mutation *in situ* shows the limitations of reductionism. *The Journal of Physiology*, **586**: 2821.

Martinovic, D., Villeneuve, D. L., Kahl, M. D., Blake, L. S., Brodin, J. D., and Ankley, G. T., 2009. Hypoxia alters gene expression in the gonads of zebrafish (*Danio rerio*). *Aquatic Toxicology*, **95**: 258-272.

Mizbani, A., Luca, E., Rushing, E. J., and Krützfeldt, J., 2016. MicroRNA deep sequencing in two adult stem cell populations identifies miR-501 as a novel regulator of myosin heavy chain during muscle regeneration. *Development*, **143**: 4137-4148.

Mohapatra, S. D., Chakrapani, V., Rasal, K. D., Barman, H. K., and Subudhi, E., 2018. Characterization and expression analysis of nadh dehydrogenase (ubiquinone) iron-sulfur protein-2 in *Channa striatus* exposed to hypoxia. *Research Journal of Biotechnology*, **13**: 1-10.

Mu, Y., Li, W., Wei, Z., He, L., Zhang, W., and Chen, X., 2020. Transcriptome analysis reveals molecular strategies in gills and heart of large yellow croaker (*Larimichthys crocea*) under hypoxia stress. *Fish & Shellfish Immunology*, **104**: 304-313.

Nemtsas, P., Wettwer, E., Christ, T., Weidinger, G., and Ravens, U., 2010. Adult zebrafish heart as a model for human heart? An electrophysiological study. *Journal of Molecular and Cellular Cardiology*, **48**: 161-171.

Nitzan, T., Kokou, F., Doron-Faigenboim, A., Slosman, T., Biran, J., Mizrahi, I., *et al.*, 2019. Transcriptome analysis reveals common and differential response to low temperature exposure between tolerant and sensitive blue tilapia (*Oreochromis aureus*). *Frontiers in Genetics*, **10**: 1-11.

Olsvik, P. A., Vikeså, V., Lie, K. K., and Hevrøy, E. M., 2013. Transcriptional responses to temperature and low oxygen stress in *Atlantic salmon* studied with next-generation sequencing technology. *BMC Genomics*, **14**: 817.

Perlmann, T., 2002. Retinoid metabolism: A balancing act. *Nature Genetics*, **31**: 7-8.

Qi, D., Chen, Q., Zheng, Z., Wu, R., Xia, M., and Chao, Y., 2018. Transcriptome analysis provides insights into the adaptive responses to hypoxia of a schizothoracine fish (*Gymnocypris eckloni*). *Frontiers in Physiology*, **9**: 1-12.

Qian, B., and Xue, L., 2016. Liver transcriptome sequencing and *de novo* annotation of the large yellow croaker (*Larimichthy crocea*) under heat and cold stress. *Marine Genomics*, **25**: 95-102.

Saetan, W., Tian, C., Yu, J., Lin, X., He, F., Huang, Y., *et al*., 2020. Comparative transcriptome analysis of gill tissue in response to hypoxia in silver sillago (*Sillago sihama*). *Animal*, **10**: 628.

Silva-Marrero, J. I., Sáez, A., Caballero-Solares, A., Viegas, I., Almajano, M. P., Fernández, F., *et al*., 2017. A transcriptomic approach to study the effect of longterm starvation and diet composition on the expression of mitochondrial oxidative phosphorylation genes in gilthead sea bream (*Sparus aurata*). *BMC Genomics*, **18**: 1-16.

Stelzle, D., Shah, A. S. V., Anand, A., Strachan, F. E., Chapman, A. R., Denvir, M. A., *et al*., 2018. High-sensitivity cardiac troponin I and risk of heart failure in patients with suspected acute coronary syndrome: A cohort study. *European Heart Journal–Quality of Care and Clinical Outcomes*, **4**: 36-42.

Hakimelahi, M., Motlagh, S., and Shojaei, M., 2012. Feeding habits and stomach contents of silver sillago, *Sillago sihama*, in the northern Persian Gulf. *Iranian Journal of Fisheries Sciences*, **11**: 892-901.

Tian, C., Li, Z., Dong, Z., Huang, Y., Du, T., Chen, H., *et al*., 2019. Transcriptome analysis of male and female mature gonads of silver sillago (*Sillago sihama*). *Genes*, **10**: 1-15.

Tian, C., Lin, X., Saetan, W., Huang, Y., Shi, H., Jiang, D., *et al*., 2020. Transcriptome analysis of liver provides insight into metabolic and translation changes under hypoxia and reoxygenation stress in silver sillago (*Sillago sihama*). *Comparative Biochemistry and Physiology–Part D: Genomics and Proteomics*, **36**: 100715.

Tongnunui, P., Sano, M., and Kurokura, H., 2010. Juvenile morphology and occurrence of two sillaginid fishes, *Sillago intermedius* and *S. sihama*, in a surf zone, southwestern Thailand. *Rajamangala University of Technology*, **2**: 1-15.

Trapnell, C., Williams, B. A., Pertea, G., Mortazavi, A., Kwan, G., van Baren, M. J., *et al*., 2010. Transcript assembly and quantification by RNA-Seq reveals unannotated transcripts and isoform switching during cell differentiation. *Nature Biotechnology*, **28**: 511.

Varet, H., Brillet-Guéguen, L., Coppée, J. Y., and Dillies, M. A., 2016. SARTools: A DESeq2- and edgeR-based R pipeline for comprehensive differential analysis of RNA-Seq data. *PLoS One*, **11**: 1-8.

Wang, T., Hu, Y., Zhu, M., and Yin, S., 2020. Integrated transcriptome and physiology analysis of *Microcystis aeruginosa* after exposure to copper sulfate. *Journal of Oceanology and Limnology*, **38**: 102-113.

Wu, C. B., Liu, Z. Y., Li, F. G., Chen, J., Jiang, X. Y., and Zou, S. M., 2017. Gill remodeling in response to hypoxia and temperature occurs in the hypoxia sensitive blunt snout bream (*Megalobrama amblycephala*). *Aquaculture*, **479**: 479-486.

Wu, S., Li, R.W., Li, W., and Li, C. J., 2012. Transcriptome characterization by RNA-seq unravels the mechanisms of butyrate-induced epigenomic regulation in bovine cells. *PLoS One*, **7**: e36940-e36940.

Xia, J. H., Liu, P., Liu, F., Lin, G., Sun, F., Tu, R., *et al*., 2013. Analysis of stress-responsive transcriptome in the intestine of asian seabass (*Lates calcarifer*) using RNA-seq. *DNA Research*, **20**: 449-460.

Yoshioka, M., 2000. Effects of temperature and salinity on hatching success of japanese whiting *Sillago japonica* eggs. *Aquaculture Science*, **48**: 637-642.

Zhang, N., Du, W., Wang, Z., Huang, Y., Du, T., and Dong, Z., 2018. Screening of reference genes for real-time PCR in different tissues from *Sillago sihama*. *Journal of Guangdong Ocean University*, **38** (5): 8-14.

Zhou, C., Lin, H., Huang, Z., Wang, J., Wang, Y., and Yu, W., 2019. Transcriptome analysis reveals differential gene expression in *Lateolabrax maculatus* following waterborne Zn exposure. *Aquaculture Reports*, **15**: 100229.

(Edited by Qiu Yantao)